Golukhova E. Z.[1], Slivneva I. V.[1], Rybka M. M.[1], Mamalyga M. L.[1], Marapov D. I.[2], Klyuchnikov I. V.[1], Antonova D. E.[1], Dibin D. A.[1]

[1] A.N. Bakulev National Medical Scientific Center for Cardiovascular Surgery, Moscow, Russia
[2] Kazan state medical Academy affiliate of the Russian medical Academy of continuing professional education, Kazan, Russia

Right ventricular systolic dysfunction as a predictor of adverse outcome in patients with COVID-19

Aim	To analyze survival of patients with COVID-19 based on echocardiographic (EchoCG) criteria for evaluation of the right ventricular (RV) systolic function.
Material and methods	Data of patients were retrospectively evaluated at the Center for Medical Care of Patients with Coronavirus Infection. Among 142 primarily evaluated patients with documented COVID-19, 110 patients (men/women, 63/47; mean age, 62.3±15.3 years) met inclusion/exclusion criteria. More than 30 EchoCG parameters were analyzed, and baseline data (comorbidities, oxygen saturation, laboratory data, complications, outcomes, etc.) were evaluated. ROC-analysis was used for evaluating the diagnostic significance of different EchoCG parameters for prediction of a specific outcome and its probability. Dependence of the overall survival of patients on different EchoCG parameters was analyzed with the Cox proportional hazards model. For assessing the predictive value of EchoCG parameters for patient stratification by risk of an adverse outcome, a predictive model was developed using the CHAID method.
Results	The in-hospital death rate of patients included into the study was 15.5%, and the death rate for this period of in-hospital observation was 12%. Based on the single-factor analysis of EchoCG parameters, a multifactor model was developed using the method of Cox regression. The model included two predictors for an unfavorable outcome, estimated pulmonary artery systolic pressure (EPASP) and maximal indexed right atrial volume (RAi), and a preventive factor, right ventricular global longitudinal strain (LS RV). Base risks for fatal outcome were determined with an account of the follow-up time. According to the obtained values, an increase in EPASP by 1 mm Hg was associated with increases in the risk of fatal outcome by 8.6% and in the RA (i) volume by 1 ml/5.8%. LS RV demonstrated an inverse correlation; a 1% increase in LS RV was associated with a 13.4% decrease in the risk for an unfavorable outcome. According to the ROC analysis, the most significant determinants of the outcome were the tricuspid annular plane systolic excursion (TAPSE) (AUC, 0.84 ± 0.06; cut-off, 18 mm) and EPASP (AUC, 0.86 ± 0.05; cut-off, 42 mm Hg). Evaluating the effects of different EchoCG predictors, that characterized the condition of the right heart, provided a classification tree. Six final decisions were determined in the model, two of which were assigned to the category of reduced risk for fatal outcome and four were assigned to the category of increased risk. Sensitivity of the classification tree model was 94.1% and specificity was 89.2%. Overall diagnostic significance was 90.0±2.9%.
Conclusion	The presented models for statistical treatment of EchoCG parameters reflect the requirement for a comprehensive analysis of EchoCG parameters based on a combination of standard methods for EchoCG evaluation and current technologies of noninvasive visualization. According to the study results, the new EchoCG marker, LS RV, allows identifying the signs of right ventricular dysfunction (particularly in combination with pulmonary hemodynamic indexes), may enhance the early risk stratification in patients with COVID-19, and help making clinical decisions for patients with different acute cardiorespiratory diseases.

Keywords	COVID-19; echocardiography; right ventricular longitudinal strain; LS RV STE; survival analysis
For citation	Golukhova E.Z., Slivneva I.V., Rybka M.M., Mamalyga M.L., Marapov D.I., Klyuchnikov I.V. et al. Right ventricular systolic dysfunction as a predictor of adverse outcome in patients with COVID-19. Kardiologiia. 2020;60(11):16–29. [Russian: Голухова Е.З., Сливнева И.В., Рыбка М.М., Мамалыга М.Л., Марапов Д.И., Ключников И.В. и др. Кардиология. 2020;60(11):16–29]

Corresponding author Slivneva I. V. E-mail: slivneva@mail.ru

Introduction

Acute lung injury caused by SARS-CoV-2 has a wide range of clinical manifestations, from mild cases to severe pneumonia. In turn, the latter can be complicated by an increased systemic inflammatory response, leading to acute respiratory distress syndro-

ISSN 0022-9040. Kardiologiia. 2020;60(11). DOI: 10.18087/cardio.2020.11.n1303

me, multiple organ system failure, and death [1–4]. The rapid development and unpredictable course of COVID-19 can lead to sudden decompensation [5] and the development of right ventricular failure.

According to some authors [6, 7], the viral agent targets not only the pulmonary tissue and microcirculation, but also directly the myocardium, causing the damages of various severity. Other authors [8, 9] consider myocardial damage a complication of COVID-19 resulting from the body's increased systemic response [10]. Nevertheless, even without direct viral effects on the myocardium, the right ventricle (RV) appears to be subjected to disproportionately strong effects when SARS-CoV-2 affects human homeostasis [11]. The non-invasive echocardiogram allows timely detection of right heart hypoperfusion, which often occurs in disturbed coronary flow or venous outflow [12], and estimation and monitoring various morphological and functional abnormalities in RV dysfunction with the impaired pulmonary flow.

However, the use of the standard protocol of generally accepted echocardiogram parameters has limited informative value. This is due to the complex geometry of RV and the inability to quickly adapt the form to hemodynamic changes arising from the progression of COVID-19 [13]. Thus, the detection and stratification of risk based on the basic echocardiographic parameters may be limited [14], especially at the early stage of the disease. 2D speckle tracking is a spatial technique used to track myocardial motion, and allows a more accurate evaluation of its function [15, 16] due to the ability to detect subclinical abnormalities in cardiac function. 2D STE is widely used to examine RV in various clinical settings [17, 18]. It is hypothesized that subtle changes in RV function may be important markers and even predictors of the clinical course of COVID-19 [11]. Current

Table 1. Clinical characteristics of patients with COVID-19 based on disease outcome

Parameter	General cohort (n=110)	Survivors (n=93)	Deceased (n=17)	p
Demographic differences				
Age. completed years (M±SD)	62.9±15.3	61.6±14.9	70.1±16.2	0.035
Male. n (%)	63 (57.3)	53 (57.0)	10 (58.8)	1.000
Female. n (%)	47 (42.7)	40 (43.0)	7 (41.2)	
BSA. m^2 (Me [Q1–Q3])	2.01 [1.86–2.13]	1.99 [1.87–2.10]	2.03 [1.84–2.18]	0.738
Systolic pressure. mmHg (Me [Q1–Q3])	125.0 [117.0–130.0]	125.0 [116.0–130.0]	125.0 [119.0–133.0]	0.724
Diastolic pressure. mmHg (Me [Q1–Q3])	77.5 [70.0–80.0]	78.0 [70.0–82.0]	70.0 [65.0–80.0]	0.129
Heart rate. bpm (Me [Q1; Q3])	79 [68.5–88.0]	79.0 [68.0–86.0]	86.0 [70.0–90.0]	0.391
Sinus rhythm. n (%)	89 (80.9)	79 (84.9)	10 (58.8)	0.019
Atrial fibrillation. n (%)	18 (16.4)	12 (12.9)	6 (35.3)	0.033
Pacemaker. n (%)	3 (2.7)	2 (2.2)	1 (5.9)	0.399
NEWS (Me [Q1–Q3])	6.0 [5.0–7.0]	6.0 [5.0–7.0]	7.0 [6.0–8.0]	0.047
SpO_2 at admission to the COVID center. % (Me [Q1–Q3])	92 [91–93]	93 [92–93]	90 [86–92]	0.002
Smokers. n (%)	4 (3.6)	4 (4.3)	0	1.000
Concomitant diseases				
Diabetes mellitus, n (%)	20 (18.2)	16 (17.2)	4 (23.5)	0.508
Bronchial asthma, n (%)	9 (8.2)	6 (6.5)	3 (17.6)	0.143
COPD, n (%)	12 (10.9)	9 (9.7)	3 (17.6)	0.393
Chronic kidney disease, n (%)	8 (7.3)	6 (6.5)	2 (11.8)	0.607
Hypertension, n (%)	81 (73.6)	66 (71.0)	15 (88.2)	0.230
CVA, n (%)	14 (12.7)	8 (8.6)	6 (35.3)	0.008
Discirculatory encephalopathy, n (%)	15 (13.6)	10 (10.8)	5 (29.4)	0.055
Cancer, n (%)	18 (16.4)	16 (17.2)	2 (11.8)	0.734
Rheumatoid arthritis, n (%)	3 (2.7)	1 (1.1)	2 (11.8)	0.062
Laboratory data				
Monocytes, $\times 10^9$/L (Me [Q1–Q3])	0.48 [0.34–0.63]	0.49 [0.34–0.63]	0.45 [0.35–0.63]	0.908
Neutrophils, $\times 10^9$/L (Me [Q1–Q3])	4.78 [3.16–6.68]	4.70 [3.16–6.63]	6.07 [3.42–8.47]	0.270
Lymphocytes, $\times 10^9$/L (Me [Q1–Q3])	1.11 [0.84–1.46]	1.15 [0.92–1.54]	0.89 [0.60–1.13]	0.011
D-dimer, ng/L (Me [Q1–Q3])	581 [342–1062]	572 [342–859]	1614 [385–3187]	0.048
Hemoglobin, g/L (Me [Q1–Q3])	139.5 [129.7–147.3]	140.3 [131.0–148.1]	130.9 [116.1–142.1]	0.088
Red blood cells, $\times 10^{12}$/L (Me [Q1–Q3])	4.82 [4.47–5.09]	4.83 [4.48–5.09]	4.63 [4.36–5.06]	0.335

Table 1 (continued). Clinical characteristics of patients with COVID-19 based on disease outcome

Parameter	General cohort (n=110)	Survivors (n=93)	Deceased (n=17)	p
White blood cells, $\times 10^9$/L (Me [Q1–Q3])	6.94 [4.7–9.5]	6.6 [4.9–9.2]	9.5 [4.0–11.8]	0.169
C-reactive protein, mg/L (Me [Q1–Q3])	6.75 [3.3–29.0]	5.5 [2.4–9.3]	76.8 [35.3–116.2]	<0.001
Platelets, $\times 10^9$/L (Me [Q1–Q3])	205.1 [156.6–255.7]	213.5 [164.2–260.4]	148.8 [119.1–198.1]	0.004
Lactate dehydrogenase, U/L (Me [Q1–Q3])	299.5 [235–422]	288 [227–387]	422 [298–665]	<0.001
Severity of pulmonary tissue damage				
Volume of pulmonary damage (CT), % (Me [Q1–Q3])	40.0 [32.0–56.0]	36.0 [28.0–48.0]	80.0 [64.0–92.0]	<0.001
Oxygen demand				
Oxygen therapy up to 10–15 L/min, n (%)	81 (73.6)	81 (87.1)	0	<0.001
High-flow oxygen therapy (AIRVO), n (%)	5 (4.5)	5 (5.4)	0	1.000
Non-invasive ventilation, n (%)	5 (4.5)	5 (5.4)	0	1.000
Invasive ventilation, n (%)	19 (17.3)	2 (2.2)	17 (100)	<0.001
ECMO, n (%)	4 (3.6)	0	4 (23.5)	<0.001
Efferent methods				
Plasmapheresis, n (%)	5 (4.5)	2 (2.2)	3 (17.6)	0.026
Hemosorption, n (%)	5 (4.5)	2 (2.2)	3 (17.6)	0.026
Complications				
Brain swelling, n (%)	3 (2.7)	0	3 (17.6)	0.003
Acute renal injury, n (%)	5 (4.5)	1 (1.1)	4 (23.5)	0.002
Acute heart failure, n (%)	13 (11.8)	2 (2.2)	11 (41.2)	<0.001
Respiratory distress syndrome, n (%)	14 (12.7)	1 (1.1)	13 (76.5)	<0.001
Multiple organ system failure, n (%)	10 (9.1)	1 (1.1)	9 (52.9)	<0.001
Gastrointestinal bleeding, n (%)	1 (0.9)	0	1 (5.9)	0.155
Hemorrhagic stroke, n (%)	1 (0.9)	1 (1.1)	0	1.000
Venous thrombosis, n (%)	11 (10.0)	9 (9.7)	2 (11.8)	0.678
DIC syndrome, n (%)	4 (3.6)	0	4 (23.5)	<0.001
Systemic inflammatory response syndrome, n (%)	14 (12.7)	5 (5.4)	9 (52.9)	<0.001

BSA. body surface area; COPD. chronic obstructive pulmonary disease;
CVA. cerebrovascular accident. CT. computed tomography; ECMO. extracorporeal membrane oxygenation;
DIC. disseminated intravascular coagulation.

non-invasive imaging techniques, one being non-Doppler strain imaging, have demonstrated benefits in monitoring RV performance [14]. Therefore, strain analysis can be used in a clinical examination algorithm focusing on preventing the progression of RV dysfunction in patients with COVID-19.

Objective

This study's objective was to determine the echocardiographic predictors of adverse outcomes and assess the predictive value of various parameters in stratifying patients by risk.

Materials and methods

A retrospective study was performed in the Healthcare Center for Patients with Coronavirus Disease (COVID center). The local ethics committee of the COVID center approved the project. All patients underwent computed tomography (CT), comprehensive echocardiogram, and a complex of laboratory tests at baseline and throughout the study. The primary analysis included 142 patients with confirmed COVID-19. Exclusion criteria were signs of left ventricular (LV) systolic dysfunction (ejection fraction<50% and/or presence of the areas of myocardial asynergy), history of myocardial infarction, aortic and mitral valve defects, history of heart surgery, pulmonary damage<25% (CT-1), pulmonary embolism, suboptimal imaging, unstable hemodynamics at the time of examination. Thus, 110 patients were included in the final analysis (63 male and 47 female patients, mean age 62.3±15.3 years). The main characteristics of the patients are provided in Table 1.

Clinical data

Arterial hypertension (73.6%), type 2 diabetes mellitus (18.2%), and cancer (16.4%) were the most

ISSN 0022-9040. Kardiologiia. 2020;60(11). DOI: 10.18087/cardio.2020.11.n1303

common concomitant pathologies in the general cohort (Table 1). The vast majority of patients had sinus rhythm (80.9%) and average heart rate (HR) of 79 bpm (Q1 – Q3: 68.5–88.0 bpm). Persistent atrial fibrillation was observed in 16.4% of cases; 2.7% of patients (n=3) had had a pacemaker implanted.

The 56-day hospital mortality of the included patients was 15.5% (n=17). In this period, the total hospital mortality was 12%. Table 1 provides the results of a comparative intergroup analysis of patients that revealed statistically significant variables associated with in-hospital death.

In the fatal outcome group, patients differed statistically significantly by age 70.1±16.2 years and NEWS score 7 (Q1 – Q3: 6–8), SpO_2 at admission 90% (Q1 – Q3: 86–92%). The most common medical history factor among deceased patients was history of cerebrovascular disorder (35.3%).

Moreover, laboratory tests showed decreased lymphocyte counts by 22.6% and platelets by 30.5%, and increased D-dimer levels 2.8-fold, C-reactive protein 13.9-fold, and lactate dehydrogenase 1.5-fold in the deceased patients compared to survivors.

The treatment protocol included antiviral, anti-inflammatory, symptomatic, anticoagulant, antiplatelet agents, bacterial infection prevention, and respiratory support.

Patients were managed until the discharge from hospital; 10% of patients were transferred to other hospitals. The median follow-up period was 13 days (Q1 – Q3: 11–17 days). The median period from onset to hospitalization was 8 days (Q1 – Q3: 6–11 days). The median time to echocardiogram was 7 days (Q1 – Q3: 4–11 days). (Table 2).

Echocardiogram analysis

Transthoracic echocardiogram was performed using a Vivid E9 (GE Healthcare) ultrasound system. The quantitative measurements were made following the guidelines of the American Society of Echocardiography and the European Association of Cardiovascular Imaging (ASE and EACVI, 2015) [19]. Two operators analyzed cine loops and images in the absence of clinical data.

Standard views (parasternal, subcostal, and apical) and modified positions were used for right heart imaging and evaluation. LV contractile function and volume characteristics were measured using the Simpson algorithm. The left and right heart's dimensional and volumetric measurements were made in the apical four-chamber view, and the corresponding indices were calculated.

LV diastolic function was evaluated by transmitral flow using pulsed-wave (PW) Doppler (E/A) and peak velocity E. With E/A=0.8 and E>50 cm/sec or E/A >0.8 and <2, additional measurements were required, including peak tricuspid regurgitation velocity, E/e′ ratio, and the maximum left atrial (LA) volume (i) (2D) [20].

Tissue Doppler imaging was used to estimate mitral annular velocity (e′). Moreover, the ratio of transmitral velocity E to the averaged early diastolic septal and lateral mitral velocity (e′) E/e′ was calculated.

Right ventricular dysfunction (2D echocardiogram) was determined using RV fractional area change (RVFAC) and tricuspid annular plane systolic excursion (TAPSE). RVFAC in the apical four-chamber view was calculated using the following formula:

$$\text{FAC RV (\%)} = (\text{EDA RV} - \text{ESA RV}) / \text{EDA RV, multiplied by 100\%,}$$

where RVEDA is RV end-diastolic area, and RVESA is RV end-systolic area. TAPSE was estimated in the M-mode.

The RV Tei index was calculated using PW and tissue Doppler imaging (TDI) and the following formulas [21, 22]:

Table 2. Characteristics of hospital stay

Parameter	General cohort (n=110)	Survivors (n=93)	Deceased (n=17)	p
Time from the disease onset, days (Me [Q1–Q3])	8 [6–11]	8 [6–11]	9 [6-10]	0.533
Admission to ICU, n (%)	11 (10.0)	5 (5.4)	6 (35.3)	0.002
Admission to a specialized unit, n (%)	99 (90.0)	88 (94.6)	11 (64.7)	
Transfer to ICU, n (%)	21 (19.1)	10 (10.8)	11 (64.7)	<0.001
Number of inpatient days, days (Me [Q1–Q3])	13 [11–17]	13 [12–16]	12 [8–17]	0.320
Number of days in ICU, days (Me [Q1–Q3])	0 [0–5]	1 [0–3]	9 [7–13]	<0.001

ICU, intensive care unit.

Figure 1. Measuring RVLS in the 2D STE mode

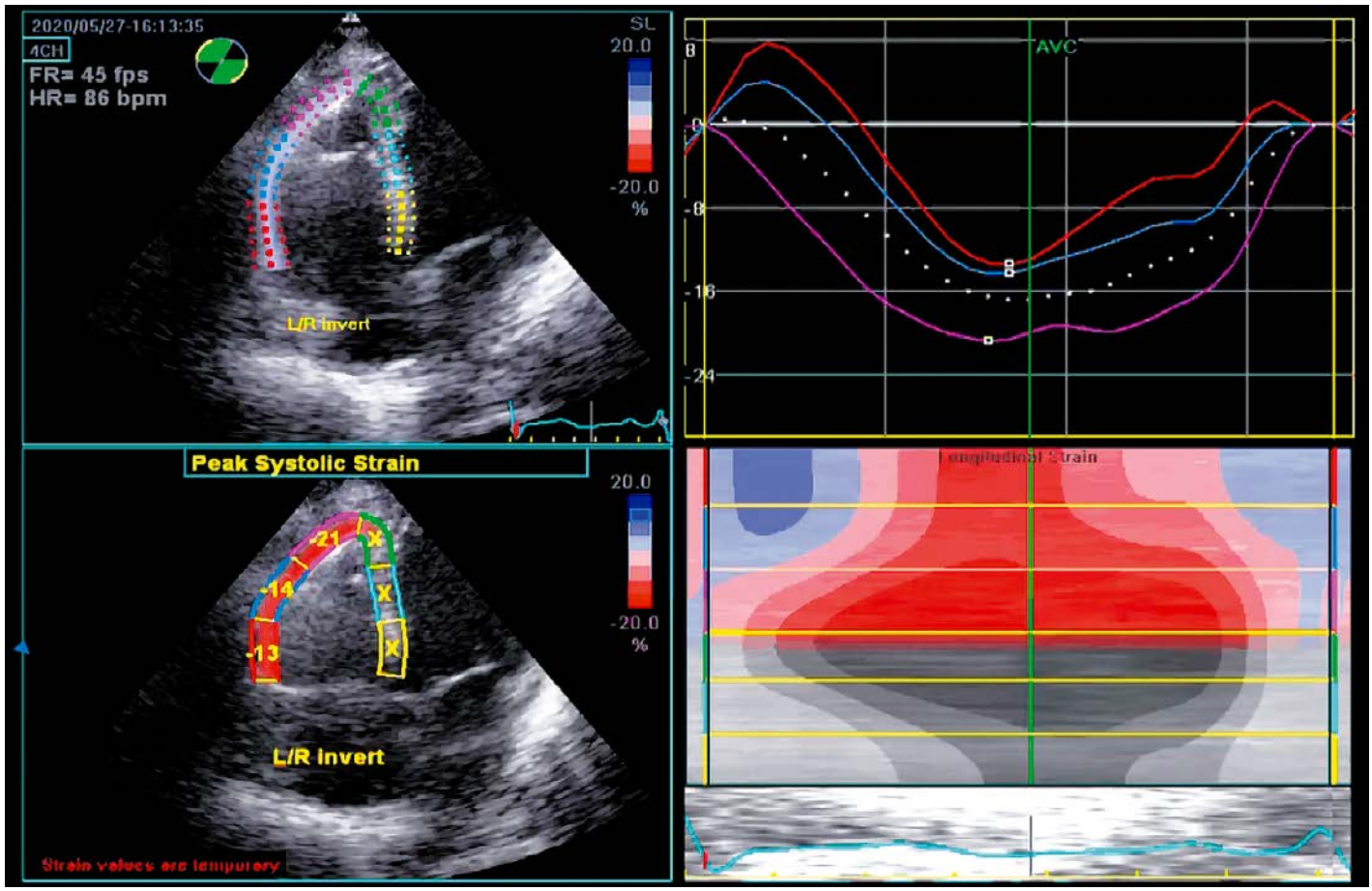

The mean longitudinal strain of the three RV free wall segments (RVLS) is 16.0%.

$$Tei = \frac{TCOT\text{-}RVET}{RVET} = \frac{IVRT+IVCT}{RVET},$$

where TCOT is tricuspid valve closure-opening time; IVRT is isovolumetric relaxation time; IVCT is isovolumetric contraction time; RVET is RV ejection time.

Systolic tricuspid annular velocity (S′) was evaluated in the PW mode.

For the analysis of RV free-wall longitudinal strain (RVLS) 2D STE, RV was recorded in the AFI (automatic functional imaging) mode based on the 2D strain function, in the apical view, and at the rate of>60 fps. The region of interest was selected, and RV wall thickness was adjusted. Six segments (three segments of RV free wall: basal, middle, apical; and similarly, three segments of the interventricular septum) were chosen (Figure 1). Septal segments were excluded from the analysis as the LV components. Following the ASE and EACVI guidelines (2015) [19, 23], absolute strain values were used, that is, non-negative numbers.

Tricuspid regurgitation flow was estimated in the color Doppler mode, and flow density and closed contour in the continuous wave mode. The intensity of tricuspid regurgitation ranged according to its significance: up to the 2nd degree and ≥2nd degree.

Pulmonary artery systolic pressure (PASP) was derived from the peak tricuspid regurgitation velocity using the modified Bernoulli equation with the right atrial (RA) pressure [22]. The mean pulmonary artery pressure (mPAP) was determined using the early diastolic peak velocity of pulmonary regurgitation (PR) using the method proposed by Masuyama et al. [24], with central venous pressure (CVP) added:

$$mPAP=4 \times LA\ peak\ velocity^2 + RA\ pressure\ (CVP).$$

The estimated RA pressure was determined by measuring its maximum diameter and the inferior vena cava (INC) caliber. Suboptimal imaging did not allow calculating mPAP in 39% of patients. The main echocardiographic parameters are listed in Table 3.

Statistical processing

Baseline information was arranged in a Microsoft Office Excel 2016 spreadsheet. Statistical analysis was

ISSN 0022-9040. Kardiologiia. 2020;60(11). DOI: 10.18087/cardio.2020.11.n1303

Table 3. Echocardiographic characteristics of patients with COVID-19 based on disease outcome

Parameter	General cohort (n=110)	Survivors (n=93)	Deceased (n=17)	p
LVEDI, mL/m² (Me [Q1–Q3])	49.6 [43.2–58.1]	49.3 [43.2–56.6]	51.4 [43.7–68.3]	0.370
LVESI, mL/m² (Me [Q1–Q3])	17.1 [14.3–22.3]	16.7 [14.2–22.1]	18.0 [15.2–28.7]	0.239
LVSVI, mL/m² (M±SD)	33.0±8.0	32.8±7.5	34.0±11.0	0.681
LVEF (2D Simpson), % (Me [Q1–Q3])	65.0 [60.0–68.0]	65.0 [60.0–69.0]	63.0 [58.0–65.0]	0.116
Minute volume, L/min (Me [Q1–Q3])	4.65 [3.91–6.26]	4.62 [3.91–6.13]	5.69 [4.26–7.23]	0.307
Cardiac index, L/min/m² (Me [Q1 – Q3])	2.44 [2.01–3.20]	2.39 [2.00–3.09]	3.02 [2.19–3.71]	0.171
E/A (Me [Q1–Q3])	1.00 [0.80–1.28]	0.94 [0.79–1.20]	1.40 [1.02–1.87]	0.009
E/e′ (Me [Q1–Q3])	7.72 [6.15–9.80]	7.56 [6.00–9.14]	9.87 [8.40–12.29]	0.001
RV/LV area (M±SD)	0.67±0.17	0.65±0.13	0.78±0.28	0.004
LA diameter, small, mm (M±SD)	39.7±5.0	39.5±4.7	41.3±6.6	0.171
LA diameter, large, mm (Me [Q1–Q3])	52.0 [49.0–58.0]	52.0 [48.5–56.0]	60.0 [52.5–61.0]	0.014
LA volume, maximum (i) (2D), mL/m² (Me [Q1–Q3])	22.3 [19.1–28.8]	21.6 [19.1–28.7]	25.6 [21.9–31.0]	0.088
RA diameter, small, mm (M±SD)	42.6±6.6	42.0±6.6	46.2±5.3	0.015
RA diameter, large, mm (Me [Q1–Q3])	52.0 [47.0–56.0]	51.0 [47.0–55.0]	56.0 [51.0–61.0]	0.004
RA volume, maximum (i) (2D), mL/m² (M±SD)	28.7±11.9	26.9±10.0	39.0±16.6	0.011
RV diameter, basal, mm (M±SD)	41.0±5.5	40.4±5.3	44.6±5.5	0.005
RV diameter, median, mm (Me [Q1–Q3])	35.0 [30.0–39.0]	34.0 [30.0–39.0]	36.5 [33.0–41.5]	0.156
RV longitudinal axis, mm (Me [Q1–Q3])	60.0 [57.0–66.0]	60.0 [57.0–66.0]	64.0 [61.0–69.0]	0.119
RV inlet, mm (Me [Q1–Q3])	33.0 [30.0–36.0]	33.0 [30.0–36.0]	35.0 [31.0–36.0]	0.476
RV outlet, mm (Me [Q1–Q3])	31.0 [28.0–33.0]	31.0 [28.0–33.0]	32.0 [28.5–35.0]	0.325
PA trunk diameter, mm (M±SD)	25.2±3.3	25.0±3.2	26.0±3.8	0.257
TR grade ≥2, n (%)	21 (19.6)	14 (15.4)	7 (43.7)	0.015
RV wall thickness (subcostal), mm (Me [Q1–Q3])	5.0 [4.0–6.0]	5.0 [4.0–6.0]	6.0 [5.0–6.0]	0.009
IVS thickness, mm (Me [Q1–Q3])	14.0 [12.0–16.0]	13.5 [12.0–16.0]	15.0 [13.0–16.5]	0.215
LV posterior wall thickness, mm (Me [Q1–Q3])	11.0 [10.0–12.0]	11.0 [10.0–12.0]	12.0 [11.0–13.0]	0.082
RV systolic function				
RVFAC (2D), % (M±SD)	51.6±10.4	52.7±10.2	45.4±9.2	0.007
TAPSE (2D), mm (Me [Q1–Q3])	20.0 [18.0–22.0]	20.0 [19.0–22.0]	16.0 [16.0–19.0]	<0.001
Tei RV (PW) (Me [Q1–Q3])	0.42 [0.32–0.58]	0.43 [0.32–0.58]	0.41 [0.34–0.74]	0.813
Tei RV (TDI) (Me [Q1–Q3])	0.57 [0.45–0.73]	0.56 [0.43–0.71]	0.71 [0.50–1.09]	0.045
Tricuspid annular S' velocity, cm/s (M±SD)	13.2±3.0	13.5±3.0	11.6±2.5	0.015
RVLS basal, % (2D STE) (M±SD)	22.5±8.1	23.3±8.0	18.2±7.0	0.016
RVLS middle, % (2D STE) (M±SD)	21.1±7.4	21.9±7.4	17.0±6.3	0.013
RVLS apical, % (2D STE) (M±SD)	18.5±7.9	19.1±7.8	15.2±8.1	0.060
RVLS global, % (2D STE) (M±SD)	20.7±6.5	21.4±6.4	16.8±5.9	0.006
Pulmonary hypertension				
ePASP, mm Hg (M±SD)	36.0±10.6	33.7±9.2	48.0±9.3	<0.001
mPAP, mmHg (Me [Q1–Q3])	15.8 [13.0–22.0]	15.0 [11.0–20.7]	23.1 [20.0–31.0]	<0.001
IVC diameter, mm (Me [Q1–Q3])	22.0 [19.0–24.0]	22.0 [19.0–24.0]	23.5 [20.0–24.5]	0.319
Tricuspid regurgitation velocity, m/s (M±SD)	2.32±0.45	2.24±0.43	2.58±0.51	0.014

EDI, end-diastolic index; ESI, end-systolic index; SVI, stroke volume index; LVEF, left ventricular ejection fraction; RV, right ventricle; LV, left ventricle; LA, left atrium; RA, right atrium; PA, pulmonary artery; IVS, interventricular septum, TR, tricuspid regurgitation; FAC, fractional area change, TAPSE, tricuspid annular plane systolic excursion; LS, longitudinal strain, ePASP, estimated pulmonary artery systolic pressure; mPAP, mean pulmonary artery pressure; IVC, inferior vena cava.

conducted using IBM SPSS Statistics v.26 (IBM Corporation).

Quantitative indicators were estimated for distribution normality using the Shapiro-Wilk test. Data distribution histograms and asymmetry and excess indicators were analyzed. In the normal distribution of quantitative traits, the data were described using the mean (M) and standard deviation (SD). When the distribution of quantitative data sets was non-normal, the data were expressed by the median (Me) and lower and upper quartiles [Q1 – Q3]. The categorical data were described with absolute values and percentages. In the normal distribution of quantitative data sets, the Student's t-test was calculated to compare the means. The Mann-Whitney U-test was used to compare independent variables in the absence of signs of normal data distribution. The differences were considered significant with $p<0.05$.

The ROC curve analysis was used to evaluate the diagnostic significance of quantitative traits in predicting a particular outcome, including its probability, calculated using the regression model. It was used to determine the optimal cut-off value of a quantitative trait, which allowed classifying patients by the risk of outcome and had the best combination of sensitivity and specificity. The quality of the prediction model obtained using this method was estimated based on the area under the ROC curve, standard error and 95% confidence interval (CI), and statistical significance level.

A classification tree was constructed to comprehensively assess the prognostic value of various echocardiographic parameters in stratifying patients by risk of death. Chi-squared automatic interaction detection (CHAID) was used for this purpose.

The dependence of overall survival on various factors was analyzed using the Cox regression method, which implies predicting the risk of an event for the object in question and evaluating the effects of predetermined independent predictors on this risk. Risk is considered a time-dependent function.

Results

Atrial fibrillation, acute cerebrovascular accident, circulatory encephalopathy, and rheumatoid arthritis were historically significant factors in calculating the death hazard ratio (Table 4).

Respiratory distress syndrome was the most common complication in the group of deceased patients (76.5%). The percentages of multiple organ system failure and systemic inflammatory response syndrome were identical (52.9%). Acute heart failure was observed in 41.2% of cases, followed by acute renal injury, coagulopathy, brain swelling, venous thrombosis, and gastrointestinal bleeding. Veno-venous extracorporeal membrane oxygenation (ECMO) was implemented in four cases. Complications observed during the hospital stay are listed in Table 1.

Calculation of the death hazard ratio (Table 5), depending on the presence and absence of a risk factor during the hospital stay, identified statistically significant risk criteria: invasive ventilation, hemosorption and plasmapheresis, acute renal injury, acute heart failure, respiratory distress syndrome, multiple organ system failure, and systemic inflammatory response syndrome. Moreover, the patient routing

Table 4. Characteristics of the correlation between the risk of death and individual medical history factors in patients with COVID-19

Criterion	OR	p	95% CI	
			Lower limit	Upper limit
Atrial fibrillation	3.36	0.033	1.06	10.65
Diabetes mellitus	1.48	0.508	0.43	5.13
Bronchial asthma	3.11	0.143	0.70	13.88
COPD	2.00	0.393	0.48	8.31
Chronic kidney disease	1.93	0.607	0.36	10.49
Hypertension	3.07	0.230	0.66	14.34
Cerebrovascular accident	5.80	0.008	1.69	19.84
Discirculatory encephalopathy	3.46	0.039	1.01	11.86
Cancer	0.64	0.734	0.13	3.09
Rheumatoid arthritis	12.27	0.041	1.05	143.83

OR, odds ratio; 95% CI, 95% confidence interval; COPD, chronic obstructive pulmonary disease.

ISSN 0022-9040. Kardiologiia. 2020;60(11). DOI: 10.18087/cardio.2020.11.n1303

Table 5. Characteristics of the correlation between the risk of death in the presence and absence of the factor risk during hospital stay

Criterion	OR	p	95% CI	
			Lower limit	Upper limit
Invasive ventilation	9.50	<0.001	2.56	35.24
Plasmapheresis	9.75	0.026	1.49	63.62
Hemosorption	9.75	0.026	1.49	63.62
Acute renal injury	28.31	0.002	2.93	273.17
Acute heart failure	83.42	<0.001	14.96	465.03
Respiratory distress syndrome	299.00	<0.001	30.99	2885.34
Multiple organ system failure	103.50	<0.001	11.60	923.56
Venous thrombosis	1.24	0.678	0.24	6.34
Systemic inflammatory response syndrome	19.80	<0.001	5.34	73.46
Admission to a specialized unit	0.10	0.002	0.03	0.40
Admission to ICU	9.60	0.001	2.51	36.74
Transfer to ICU	15.22	<0.001	4.62	50.10

OR, odds ratio; 95% CI, 95% confidence interval; ICU, intensive care unit.

Table 6. Estimation of the effects of the predictors on the survival of patients with COVID-19

Predictor	B	HR	95% CI	p
RA diameter, small (2D)	0.09	1.09	1.01–1.18	0.026
RA diameter, large (2D)	0.14	1.15	1.06–1.24	<0.001
RA volume, maximum (i) (2D)	0.08	1.08	1.04–1.12	<0.001
RVEDD, basal (2D)	0.09	1.09	1.01–1.17	0.019
RVEDD, middle (2D)	0.08	1.08	1.01–1.16	0.034
RVFAC (2D)	–0.05	0.96	0.91–1.0	0.054
TAPSE (2D)	–0.48	0.62	0.49–0.79	<0.001
RV/LV area (2D)	2.73	15.28	1.92–121.7	0.01
RVLS basal (2D STE)	–0.07	0.93	0.87–1.0	0.045
RVLS middle (2D STE)	–0.10	0.91	0.84–0.99	0.022
RVLS distal (2D STE)	–0.08	0.93	0.86–1.0	0.051
RVLS global (2D STE)	–0.12	0.89	0.81–0.97	0.01
ePASP	0.09	1.09	1.04–1.14	<0.001
mPAP	0.11	1.12	1.05–1.18	<0.001

HR, hazard ratio at the time of t; B, value of the factor in the equation; 95% CI, 95% confidence interval; RA, right atrium; RV, right ventricle; LV, left ventricle; RVEDD, right ventricular end-diastolic dimension; FAC, fractional area change; TAPSE, tricuspid annular plane systolic excursion; LS, longitudinal strain; ePASP, estimated pulmonary artery systolic pressure; mPAP, mean pulmonary artery pressure.

options, and the risk of death were correlated: hospitalization in the ICU, transfer from the specialized unit to the ICU.

The effects of various echocardiographic predictors characterizing right heart performance on the survival of patients with COVID-19 was assessed using the Cox proportional-hazards model. The results of the univariate analysis for predictors demonstrating statistically significant effects on overall survival are presented in Table 6.

As shown in Table 6, increased RVFAC (2D), TAPSE (2D), and RVLS global (2D STE) were accom-

Table 7. Estimation of the effects of the predictors included in the model (1) on the survival of patients with COVID-19

Predictor	HR	95% CI	p
ePASP, mmHg	1.086	1.03–1.15	0.003
RA volume, maximum (i) (2D), mL/m²	1.058	1.02–1.10	0.002
RVLS global (2D STE), %	0.866	0.78–0.97	0.012

HR, hazard ratio at the time t; CI, confidence interval; ePASP, estimated calculated pulmonary artery systolic pressure; RA, right atrium; LS, longitudinal strain; RV, right ventricle.

Table 8. Baseline risk of death in patients with conditionally zero predictors included in the model (1)

Follow-up period, day	Accumulated risk of death, %
7	0.14
14	0.66
21	2.54
28	3.35
35	4.31

Figure 2. ROC curve characterizing the dependence of the probability of death: on the TAPSE values (A), on the ePASP values (B)

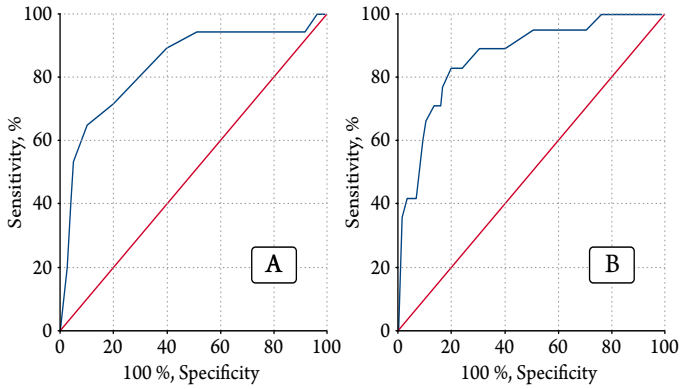

panied by a reduced risk of death. The remaining parameters listed in the table were directly correlated with the risk of death in patients with COVID-19.

Next, we attempted to combine predictors in a multivariate model that allowed predicting the risk of death in patients with COVID-19 based on the echocardiographic parameters of the right heart over time. The following model (1) was produced using the Cox regression method and selecting factors by process of elimination:

$$h_i(t) = h_0(t) \times \exp(0.082 \times X_1 + 0.057 \times X_2 - 0.143 \times X_3), \quad (1)$$

where $h_i(t)$ is the risk of death for patient i in a specific period t; $h_0(t)$ is the baseline risk of death (with a conditional zero value of all predictors included in the model) in a specific period t; X_1 is ePASP (mmHg); X_2 is the maximum RA volume (i) (2D) (mL/m²); and X_3 is global RVLS (2D STE) (%).

The resulting model was statistically significant ($p<0.001$). The effects of each predictor included in the model (1) on the probability of death in patients with COVID-19 are described in Table 7.

Values of the baseline risk of death in a patient with COVID-19, with conditionally zero values of the predictors included in the model (1), are provided in Table 8.

Given the hazard ratio (HR) values calculated, an increase in ePASP by 1 mmHg was accompanied by a 1.086-fold or 8.6% increase in the risk of death, and an increase in the RA volume index by 1 mL/m² was accompanied by a 1.058-fold or 5.8% increase in the risk of death. The global RVLS (2D STE) predictor was characterized by a reverse correlation with mortality: a 1% increase was accompanied by a 1.155-fold or 13.4% reduction in the risk of death.

ROC analysis was also performed to determine thresholds for the right heart echocardiographic parameters when predicting deaths without taking into account the duration of follow-up. See the results in Table 9.

Of all the ROC-analyzed predictors that had statistically significant effects on the probability of death in patients with COVID-19, TAPSE and ePASP had the highest AUC values.

The ROC curves describing the predictive value of TAPSE and ePASP are shown in Figure 2A and Figure 2B, respectively.

The classification tree resulted from assessing the effects of various echocardiographic predictors of right heart performance on the probability of death in patients with COVID-19 using the CHAID method (Figure 3).

The analysis allowed identifying six terminal nodes, which are characterized in Table 10.

With a total mortality rate of 15.5%, nodes 7 and 10 refer to patients at lower risk of death. Nodes 9, 4, 6, and 8 are classified as an increased risk of death, with node 4 having the highest percentage in the study population structure.

The sensitivity of the model was 94.1%, and specificity was 89.2%. The general diagnostic significance was 90.0±2.9%.

ISSN 0022-9040. Kardiologiia. 2020;60(11). DOI: 10.18087/cardio.2020.11.n1303

Table 9. Results of the analysis of ROC curves characterizing statistically significant dependence of the death probability in patients with COVID-19 on echocardiographic parameters of the right heart

Parameter	AUC	95% CI	Cut-off	Se, %	Sp, %
RA diameter, small (2D)	0.71±0.06	0.59–0.83	44 mm	76.5	63.4
RA diameter, large (2D)	0.72±0.07	0.59–0.85	54 mm	70.6	62.4
RA volume, maximum (i) (2D)	0.74±0.06	0.62–0.86	29.4 mL/m^2	75.0	64.4
RVEDD, basal (2D)	0.72±0.07	0.60–0.85	42 mm	81.3	63.4
RVFAC (2D)	0.71±0.06	0.58–0.83	50.3%	64.7	61.3
TAPSE (2D)	0.84±0.06	0.72–0.95	18 mm	70.6	81.2
RVLS global (STE)	0.71±0.07	0.58–0.85	19.6%	76.5	63.0
ePASP	0.86±0.05	0.76–0.96	42 mmHg	82.4	79.8
mPAP	0.77±0.06	0.66–0.89	19.8 mmHg	76.5	69.3

AUC, area under the ROC curve; CI, confidence interval; Se, sensitivity (%); Sp, specificity (%); cut-off, optimal cut-off point; RA, right atrium; RV, right ventricle; EDD, end-diastolic dimension; FAC, fractional area change; TAPSE, tricuspid annular plane systolic excursion; LS, longitudinal strain; ePASP, estimated pulmonary artery systolic pressure; mPAP, mean pulmonary artery pressure.

Discussion

Despite abundant information on identifying risk factors in patients with COVID-19, the identification of echocardiographic factors of RV systolic dysfunction as a predictor of adverse outcome was discussed in only one published work [14]. This is why our study included a comprehensive analysis of the diagnostic and prognostic value of various echocardiographic parameters of the right heart and developed the model to predict adverse outcomes in patients with COVID-19 treated at the COVID center.

Univariate analysis was performed using risk function simulation (Cox regression) (Table 6). Interestingly, RVFAC (2D) was not statistically significant. This may be due to the fact that RVFAC (2D) measurement is based on end-diastolic and end-systolic areas of RV, which is a single-plane RV assessment and does not appear to have the necessary information value with regard to RV performance in the presence of acute lung injury.

ROC analysis allowed finding the thresholds of the various echocardiographic parameters of the right heart without taking into account the monitoring period (Table 9). TAPSE and ePASP had the biggest areas under the curve. ePASP was highly sensitive (82.4%) and specific (79.8%) at the cut-off point of 42 mmHg. Thus, the selected cut-off point can be recommended as a threshold for predicting death risk and used in clinical decision-making for patients with COVID-19.

Identifying the echocardiographic risk factors for RV dysfunction contributed to the development of the

Table 10. Characteristics of the terminal nodes (groups) obtained from the classification of subjects

Node number	Parameter values	Node percentage in the total structure, n (%)	Mortality (%)
7	RVLS global (2D STE) ≤ 20.7% FWF, ePASP ≤ 41 mmHg, RA volume, maximum (i) (2D) ≤ 42.4 mL/m^2	33 (30.0)	0.0
10	RVLS global (2D STE)>20.7%, RV/LV area (2D) ≤0.88, TAPSE (2D) >16 mm	51 (46.4)	2.0
9	RVLS global (2D STE)>20.7%, RV/LV area (2D) ≤0.88, TAPSE (2D) ≤ 16 mm	2 (1.8)	50.0
4	RVLS global (2D STE) ≤ 20.7% FWF, ePASP >41 mmHg	17 (15.5)	58.8
6	RVLS global (2D STE)>20.7%, RV/LV area (2D)>0.88	3 (2.7)	66.7
8	RVLS global (2D STE) ≤ 20.7% ePASP ≤41 mmHg, RA volume, maximum (i) (2D) >42.4 mL/m^2	4 (3.6)	75.0

LS, longitudinal strain; ePASP, estimated pulmonary artery systolic pressure; RA, right atrium; RV, right ventricle; LV, left ventricle; TAPSE, tricuspid annular plane systolic excursion.

Figure 3. Subject classification according to the death risk based on echocardiographic predictors characterizing the right heart

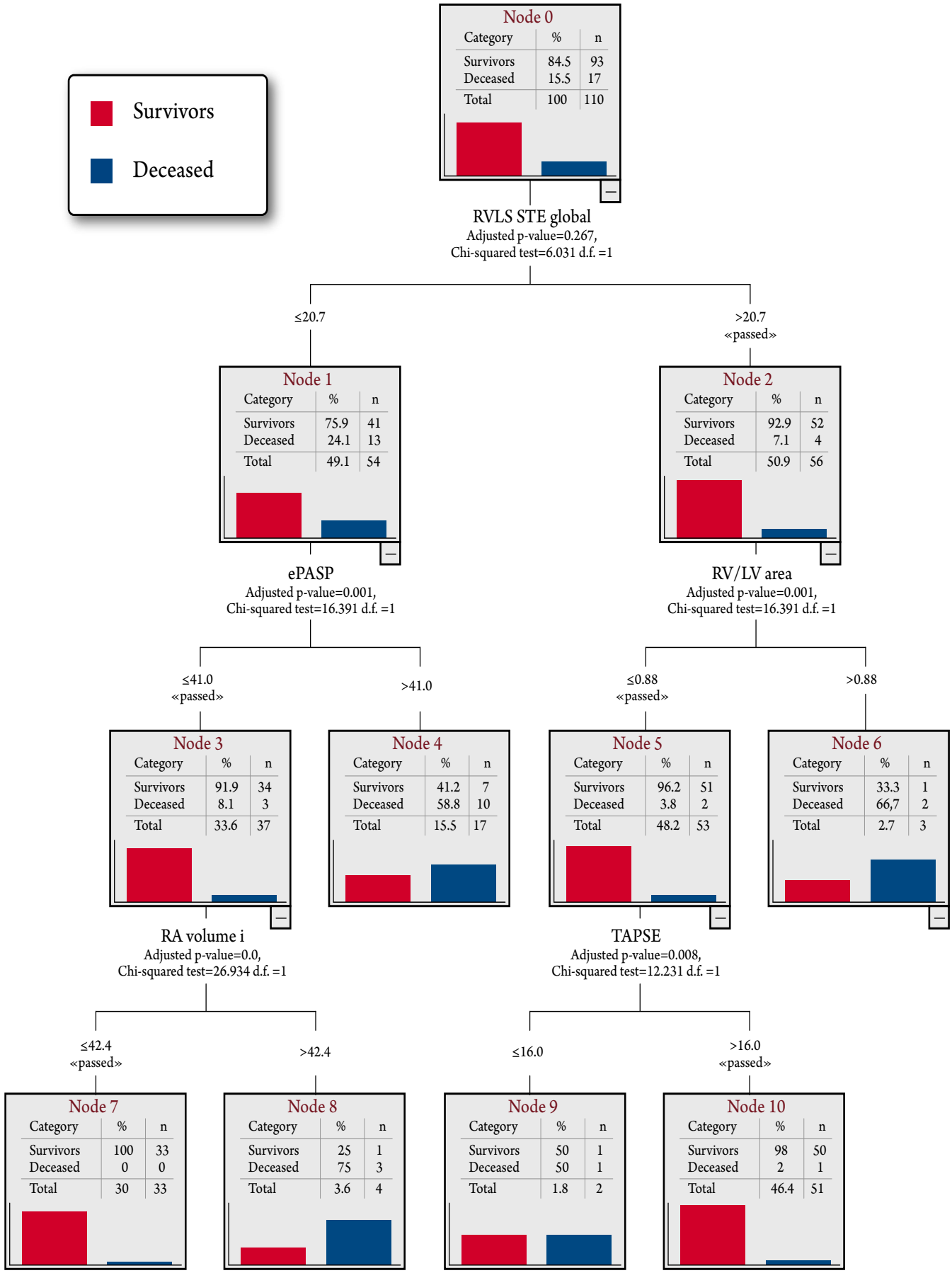

ISSN 0022-9040. Kardiologiia. 2020;60(11). DOI: 10.18087/cardio.2020.11.n1303

multivariate prediction model (1) used to predict the risk of death in patients with COVID-19 over time. It includes two risk factors for death: ePASP, maximum RA volume (i), and one preventive factor, global RVLS (2D STE) (Table 7).

The resulting model allows predicting death risk, taking into account the monitoring period (Table 8). Moreover, global RVLS (2D STE) showed good quality of the model in the univariate analysis with the cut-off point of 19.6%. However, sensitivity (76.5%) and specificity (63.0%) were not high. The predictive value of global RVLS (2D STE) was better in combination with two risk factors (ePASP, maximum RA volume [i]) in the Cox multivariate regression analysis.

CHAID allowed dividing the sample into several subgroups, each of which had a particular relation to the dependent variable, that is, performing multivariate node splitting.

A decision tree is used to present data in a hierarchical, sequential structure, in which each object has a single node providing a solution. The rule is a logical design represented as «if…, then…» The root node represents the entire sample, which is global RVLS (2D STE) used in our model. Terminal nodes are the best final solutions. In the given model (Figure 3), terminal nodes 9, 4, 6, and 8 were classified as high risk of death. Node 4 had the largest percentage in the total study structure, which was a combination of global RVLS (2D STE) ≤20.7% and ePASP >41 mmHg, identified in 15.5% (n=17) in the total cohort with 58.8% mortality.

The sensitivity of the model was 94.1%, and specificity was 89.2%. The total percentage of correctly predicted values of the dependent variable was 90.0%±2.9%. Thus, this model reflects imperfections of the univariate assessment and the need for comprehensive analysis of echocardiographic parameters based on a combination of common echocardiographic methods and modern non-invasive imaging techniques.

The longitudinal strain of the RV myocardium (RVLS 2D STE) is a spatial echocardiographic parameter that allows detecting RV changes at the early stage of the disease since pattern-tracking technology is more sensitive than visual assessment and common parameters of echocardiographic diagnosis [16]. Moreover, as shown in several studies, the longitudinal strain of RV (RVLS 2D STE) has a predictive value [14, 25–28] exceeding that of conventional echocardiogram, even in the presence of significant tricuspid regurgitation [28]. According to our results, the new echocardiographic biomarker RVLS allows identifying the signs of systolic dysfunction, especially in combination with pulmonary hemodynamic indicators, and may have additional significance in the early risk stratification of patients with COVID-19 and clinical decision-making [11].

Simplifying complex functions and common use of advanced ultrasound STE systems, including portable mobile-diagnosis devices, [29] will allow soon to extract relevant data for the classification of patients by the risk and to obtain necessary information for clinical decision-making on immediate treatment and further critical measures in patients with various acute cardiorespiratory diseases [11].

Limitations

In this study, the prediction model used to assess death risk in patients with COVID-19 included only echocardiographic parameters.

The study did not analyze the effects of lung injury according to CT, demographic, clinical, and laboratory parameters on the prognosis of adverse outcomes. The results are limited to the analysis of echocardiographic predictors that characterize the right heart.

Conclusion

Identifying echocardiographic risk factors for RV dysfunction contributed to the development of a prediction model of lethal outcome in COVID-19 depending on the duration of monitoring. It includes two risk factors for death: ePASP, maximum RA volume (i), and one preventive factor, global RVLS (2D STE).

According to the ROC analysis, TAPSE and ePASP had the biggest areas under the curve. The ePASP threshold value of 42 mmHg demonstrated high sensitivity (82.4%) and specificity (79.8%), and can be recommended to predict death risk and can be used in clinical decision-making for patients with COVID-19.

The new echocardiographic biomarker, RVLS, especially in combination with pulmonary hemodynamic indicators, allows identifying the signs of RV systolic dysfunction, which is essential in the early risk stratification of patients with COVID-19.

No conflict of interest is reported.

The article was received on 31/07/2020

REFERENCES

1. Chen N, Zhou M, Dong X, Qu J, Gong F, Han Y et al. Epidemiological and clinical characteristics of 99 cases of 2019 novel coronavirus pneumonia in Wuhan, China: a descriptive study. The Lancet. 2020;395(10223):507–13. DOI: 10.1016/S0140-6736(20)30211-7
2. Siddiqi HK, Mehra MR. COVID-19 illness in native and immunosuppressed states: A clinical-therapeutic staging proposal. The Journal of Heart and Lung Transplantation. 2020;39(5):405–7. DOI: 10.1016/j.healun.2020.03.012
3. Mehta P, McAuley DF, Brown M, Sanchez E, Tattersall RS, Manson JJ. COVID-19: consider cytokine storm syndromes and immunosuppression. The Lancet. 2020;395(10229):1033–4. DOI: 10.1016/S0140-6736(20)30628-0
4. CDC. Interim Clinical Guidance for Management of Patients with Confirmed Coronavirus Disease (COVID-19). 2020. [Internet] 2020. Available at: https://www.cdc.gov/coronavirus/2019-ncov/hcp/clinical-guidance-management-patients.html
5. Potere N, Valeriani E, Candeloro M, Tana M, Porreca E, Abbate A et al. Acute complications and mortality in hospitalized patients with coronavirus disease 2019: a systematic review and meta-analysis. Critical Care. 2020;24(1):389. DOI: 10.1186/s13054-020-03022-1
6. Inciardi RM, Lupi L, Zaccone G, Italia L, Raffo M, Tomasoni D et al. Cardiac Involvement in a Patient With Coronavirus Disease 2019 (COVID-19). JAMA Cardiology. 2020;5(7):819–24. DOI: 10.1001/jamacardio.2020.1096
7. Zhou F, Yu T, Du R, Fan G, Liu Y, Liu Z et al. Clinical course and risk factors for mortality of adult inpatients with COVID-19 in Wuhan, China: a retrospective cohort study. The Lancet. 2020;395(10229):1054–62. DOI: 10.1016/S0140-6736(20)30566-3
8. Xu Z, Shi L, Wang Y, Zhang J, Huang L, Zhang C et al. Pathological findings of COVID-19 associated with acute respiratory distress syndrome. The Lancet Respiratory Medicine. 2020;8(4):420–2. DOI: 10.1016/S2213-2600(20)30076-X
9. Shi S, Qin M, Shen B, Cai Y, Liu T, Yang F et al. Association of Cardiac Injury Ц1th Mortality in Hospitalized Patients With COVID-19 in Wuhan, China. JAMA Cardiology. 2020;5(7):802–10. DOI: 10.1001/jamacardio.2020.0950
10. Singh R, Kashyap R, Hutton A, Sharma M, Surani S. A Review of Cardiac Complications in Coronavirus Disease 2019. Cureus. 2020;12(5): e8034. DOI: 10.7759/cureus.8034
11. Minardi J, Marsh C, Sengupta P. Risk-Stratifying COVID-19 Patients the Right Way. JACC Cardiovascular Imaging. 2020;13(11):2300-2303. doi: 10.1016/j.jcmg.2020.05.012
12. Greyson CR. Pathophysiology of right ventricular failure: Critical Care Medicine. 2008;36(1 Suppl):S57–65. DOI: 10.1097/01.CCM.0000296265.52518.70
13. Haddad F, Hunt SA, Rosenthal DN, Murphy DJ. Right Ventricular Function in Cardiovascular Disease, Part I: Anatomy, Physiology, Aging, and Functional Assessment of the Right Ventricle. Circulation. 2008;117(11):1436–48. DOI: 10.1161/CIRCULATIONAHA.107.653576
14. Li Y., Li H., Zhu S, Xie Y, Wang B, He L et al. Prognostic Value of Right Ventricular Longitudinal Strain in Patients with COVID-19. JACC Cardiovasc Imaging. 2020;13(11):2287-2299. DOI: 10.1016/j.jcmg.2020.04.014
15. Mor-Avi V, Lang RM, Badano LP, Belohlavek M, Cardim NM, Derumeaux G et al. Current and Evolving Echocardiographic Techniques for the Quantitative Evaluation of Cardiac Mechanics: ASE/EAE Consensus Statement on Methodology and Indications Endorsed by the Japanese Society of Echocardiography. European Journal of Echocardiography. 2011;12(3):167–205. DOI: 10.1093/ejechocard/jer021
16. Longobardo L, Suma V, Jain R, Carerj S, Zito C, Zwicke DL et al. Role of Two-Dimensional Speckle-Tracking Echocardiography Strain in the Assessment of Right Ventricular Systolic Function and Comparison with Conventional Parameters. Journal of the American Society of Echocardiography. 2017;30(10):937-946.e6. DOI: 10.1016/j.echo.2017.06.016
17. Li Y, Xie M, Wang X, Lu Q, Zhang L, Ren P. Impaired Right and Left Ventricular Function in Asymptomatic Children with Repaired Tetralogy of Fallot by Two-Dimensional Speckle Tracking Echocardiography Study. Echocardiography. 2015;32(1):135–43. DOI: 10.1111/echo.12581
18. Xie M, Li Y, Cheng TO, Wang X, Dong N, Nie X et al. The effect of right ventricular myocardial remodeling on ventricular function as assessed by two-dimensional speckle tracking echocardiography in patients with tetralogy of Fallot: A single center experience from China. International Journal of Cardiology. 2015; 178:300–7. DOI: 10.1016/j.ijcard.2014.10.027
19. Lang RM, Badano LP, Mor-Avi V, Afilalo J, Armstrong A, Ernande L et al. Recommendations for Cardiac Chamber Quantification by Echocardiography in Adults: An Update from the American Society of Echocardiography and the European Association of Cardiovascular Imaging. European Heart Journal – Cardiovascular Imaging. 2015;16(3):233–71. DOI: 10.1093/ehjci/jev014
20. Nagueh SF, Smiseth OA, Appleton CP, Byrd BF, Dokainish H, Edvardsen T et al. Recommendations for the evaluation of left ventricular diastolic function by echocardiography: an update from the American Society of Echocardiography and the European Association of Cardiovascular Imaging. Journal of the American Society of Echocardiography. 2016;29(4):277–314. DOI: 10.1016/j.echo.2016.01.011
21. Tei C, Dujardin KS, Hodge DO, Bailey KR, McGoon MD, Tajik AJ et al. Doppler echocardiographic index for assessment of global right ventricular function. Journal of the American Society of Echocardiography. 1996;9(6):838–47. DOI: 10.1016/S0894-7317(96)90476-9
22. Rudski LG, Lai WW, Afilalo J, Hua L, Handschumacher MD, Chandrasekaran K et al. Guidelines for the Echocardiographic Assessment of the Right Heart in Adults: A Report from the American Society of Echocardiography. Journal of the American Society of Echocardiography. 2010;23(7):685–713. DOI: 10.1016/j.echo.2010.05.010
23. Voigt J-U, Pedrizzetti G, Lysyansky P, Marwick TH, Houle H, Baumann R et al. Definitions for a common standard for 2D speckle tracking echocardiography: consensus document of the EACVI/ASE/Industry Task Force to standardize deformation imaging. European Heart Journal - Cardiovascular Imaging. 2015;16(1):1–11. DOI: 10.1093/ehjci/jeu184
24. Masuyama T, Kodama K, Kitabatake A, Sato H, Nanto S, Inoue M. Continuous-wave Doppler echocardiographic detection of pulmonary regurgitation and its application to noninvasive estimation of pulmonary artery pressure. Circulation. 1986;74(3):484–92. DOI: 10.1161/01.CIR.74.3.484
25. Hulshof HG, Eijsvogels TMH, Kleinnibbelink G, van Dijk AP, George KP, Oxborough DL et al. Prognostic value of right ventricular longitudinal strain in patients with pulmonary hypertension: a systematic review and meta-analysis. European Heart Journal - Cardiovascular Imaging. 2019;20(4):475–84. DOI: 10.1093/ehjci/jey120
26. Motoki H, Borowski AG, Shrestha K, Hu B, Kusunose K, Troughton RW et al. Right Ventricular Global Longitudinal Strain Provides Prognostic Value Incremental to Left Ventricular Ejection Fraction in Patients with Heart Failure. Journal of the American Society of Echocardiography. 2014;27(7):726–32. DOI: 10.1016/j.echo.2014.02.007

ISSN 0022-9040. Kardiologiia. 2020;60(11). DOI: 10.18087/cardio.2020.11.n1303

27. Da Costa Junior AA, Ota-Arakaki JS, Ramos RP, Uellendahl M, Mancuso FJN, Gil MA et al. Diagnostic and prognostic value of right ventricular strain in patients with pulmonary arterial hypertension and relatively preserved functional capacity studied with echocardiography and magnetic resonance. The International Journal of Cardiovascular Imaging. 2017;33(1):39–46. DOI: 10.1007/s10554-016-0966-1
28. Prihadi EA, van der Bijl P, Dietz M, Abou R, Vollema EM, Marsan NA et al. Prognostic Implications of Right Ventricular Free Wall Longitudinal Strain in Patients with Significant Functional Tricuspid Regurgitation. Circulation: Cardiovascular Imaging. 2019;12(3): e008666. DOI: 10.1161/CIRCIMAGING.118.008666
29. Jafari MH, Girgis H, Van Woudenberg N, Moulson N, Luong C, Fung A et al. Cardiac point-of-care to cart-based ultrasound translation using constrained CycleGAN. International Journal of Computer Assisted Radiology and Surgery. 2020;15(5):877–86. DOI: 10.1007/s11548-020-02141-y